AIP Applied Physics Letters

Identity of the light-emitting states in porous silicon wires

Chin-Yu Yeh, S. B. Zhang, and Alex Zunger

Citation: Applied Physics Letters **63**, 3455 (1993); doi: 10.1063/1.110118
View online: http://dx.doi.org/10.1063/1.110118
View Table of Contents: http://scitation.aip.org/content/aip/journal/apl/63/25?ver=pdfcov
Published by the AIP Publishing

Identity of the light-emitting states in porous silicon wires

Chin-Yu Yeh, S. B. Zhang, and Alex Zunger
National Renewable Energy Laboratory, Golden, Colorado 80401

(Received 4 June 1993; accepted for publication 17 October 1993)

We present empirical pseudopotential calculations of the electronic structure of [001] silicon quantum wires, aiming at identification of the states that couple radiatively to the valence-band maximum. We find that the near-gap wave functions differ qualitatively from effective-mass depictions. Instead, they can be described as off-Γ bulk states. The effects of H chemisorption on the wire energies and wave functions are studied. We find that the Si skeleton dominates the emission. The resulting lifetimes versus energy relation agrees with the experimental measurements only if one assumes coexistence of quantum wires with quantum dots.

Much of the current debate on porous Si[1–4] centers on the microscopic origins of its blueshifted, intense light emission. Recent experiments[5,6] suggest that the emission originates from the Si skeleton rather than from "extrinsic" states. Given the nanoscale size of the hydrogen- or oxygen-coated Si and that the surface/volume ratio is as large as ~50% one wonders how the light-emitting entity can reflect "bulklike" Si characteristics. It is also important to find out if the emission originates only from Si *wires* or also from other quantum objects, e.g., dots. We address these questions theoretically by modeling the electronic structure of clean versus hydrogen-covered silicon wires and silicon boxes.

We have calculated the band energies, transition matrix element, and radiative lifetimes of [001] Si quantum structures with (110)×(−110) faces and square cross sections ranging from 4×4 to 14×14 monolayers (7.7×7.7–26.9×26.9 Å, respectively). For a wire the z direction is infinitely long. For a box we take[7] $L_z=\sqrt{2}L_x$. We use a direct band-structure approach, solving

$$[-\tfrac{1}{2}\nabla^2+V^{\text{wire}}(\mathbf{r})]\psi_f^{\text{wire}}(\mathbf{r})=\epsilon_f^{\text{wire}}\psi_f^{\text{wire}}(\mathbf{r}), \tag{1}$$

where the wire potential $V^{\text{wire}}(\mathbf{r})$ is constructed as a superposition of atomic pseudopotentials. Equation (1) is solved by imposing artificial periodic boundary conditions on the wire straddled by N_v layers of vacuum. This transforms Eq. (1) into a Bloch-periodic band-structure problem with a giant (super) cell, solved here by expanding ψ_f^{wire} in plane waves. We use a sufficiently large wire–wire separation N_v so that the solutions become N_v independent. Effective-mass approximations are completely avoided. We consider wires with clean, unreconstructed free surfaces as well as hydrogen-coated wires where the dangling bonds are saturated. Since we are interested in the present discussion in understanding the electronic structure of *intrinsic*, bulklike states, we will not discuss the surface dangling bond states of the wire with free surface. Hydrogen chemisorption naturally removes the surface states. The empirical Si pseudopotential used was fitted to the bulk Si band structure and to the (110) surface work function (4.9 eV), while the hydrogen potential was fitted to the surface density of states of hydrogen-covered Si (001), (110), and (111) surfaces.[7] We use bulklike Si–Si distance, 2.24 Å, while the Si-H distances are 1.49 Å. Transition probabilities $P_{ff'}$ are computed from the dipole matrix elements of $\psi_f^{\text{wire}}(\mathbf{r})$ while radiative lifetimes τ_R are calculated from

$$\frac{1}{\tau_R}=\frac{2\alpha\omega n}{3m_e^2c^2}P_{ff'}, \tag{2}$$

where α is the fine structure constant, ω is the photon angular frequency, n is the refractive index[8] ($n=1.2$ for *porous* Si), m_e is the free electron mass, and c is the velocity of light.

It is useful to analyze the solutions of Eq. (1) in terms of a superposition of *bulk* states. To do so, we defined a set of *symmetrized bulk wave functions*

$$\begin{aligned}\chi_{n,\mathbf{k}}^{\text{TC}}(\mathbf{r})=N[&u_{n,k_x,k_y,k_z}e^{i\mathbf{k}(\mathbf{x}+\mathbf{y})}+\alpha_1u_{n,k_x,\bar{k}_y,k_z}e^{-i\mathbf{k}(\mathbf{x}-\mathbf{y})}\\&+\alpha_2u_{n,k_x,\bar{k}_y,k_z}e^{i\mathbf{k}(\mathbf{x}-\mathbf{y})}\\&+\alpha_3u_{n,\bar{k}_x,\bar{k}_y,k_z}e^{-i\mathbf{k}(\mathbf{x}+\mathbf{y})}]e^{ik_zz},\end{aligned} \tag{3}$$

where $u_{n,\mathbf{k}}$ is the Bloch-periodic part of the bulk wave function, N is a normalization constant, and α_i are coefficients of norm one. The quantization conditions, for a wire with lattice vectors $x=(1/\sqrt{2})(1,1,0)$ and $y=(1/\sqrt{2})(-1,1,0)$, are $\mathbf{k}_x=j_x(1,1,0)$; $\mathbf{k}_y=j_y(-1,1,0)$; (in units of $2\pi/Na_0$, where N is the number of the atomic monolayers within the wire width L, a_0 is the bulk lattice constant), and j_x, j_y are integer quantum numbers. The directly calculated wire wave functions of Eq. (1) can be expanded within the wire space in the complete set of these "truncated crystal" (TC) basis functions $\{\chi_{n,\mathbf{k}}^{\text{TC}}\}$,

$$\psi_{f,\Gamma}^{\text{wire}}(\mathbf{r})=\sum_n\sum_{k_x,k_y}a_{n,f}(k_x,k_y)\chi_{n,k_x,k_y}^{\text{TC}}(\mathbf{r}), \tag{4}$$

where $a_{n,f}(k_x,k_y)=\langle\psi_f^{\text{wire}}(\mathbf{r})|\chi_{n,k_x,k_y}^{\text{TC}}(\mathbf{r})\rangle$. We will use the projections $|a_{n,f}|^2$ to determine the identity of the directly calculated wire states in terms of bulk Si bands at (n,k_x,k_y). Recall that in the effective-mass particle-in-a-box approach, the wire states are described in terms of *band-edge*(k_0) Bloch function $u_{n,k_0}(\mathbf{r})$ and sinusoidal envelope functions, i.e.,

$$\psi_{f,\Gamma}^{\text{EMA}}(k_x,k_y)=\frac{2}{L}u_{n,k_0}(\mathbf{r})\sin(k_xx)\sin(k_yy), \tag{5}$$

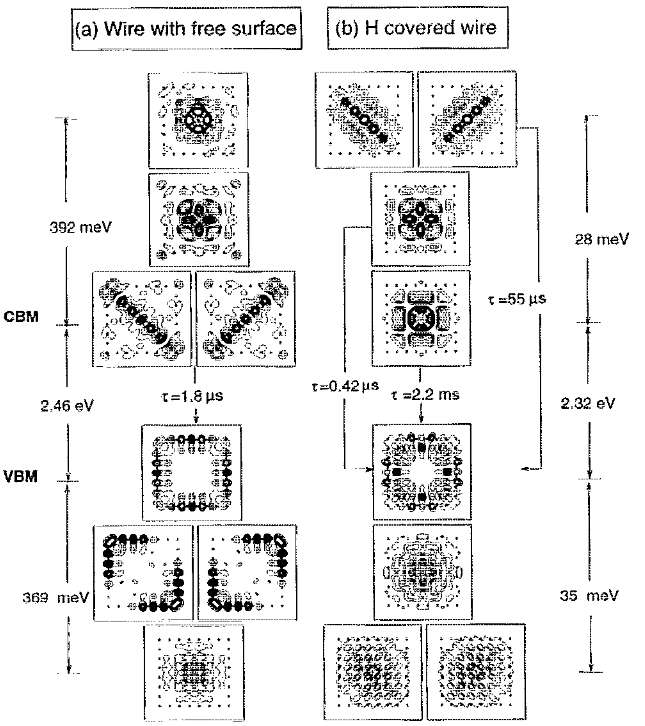

FIG. 1. z-direction averaged wave-function squares, energy separations, and lifetimes for the near band-gap states. The dots denote positions of outer Si atoms.

rather than in terms of the more general expansion of Eq. (4).

Our results can be summarized as follows.

(i) *The near band-gap wire states are linear combinations of off-Γ bulk states, not effective masslike states:* The projections of Eqs. (3) and (4) shows that 90% of the valence-band maximum (VBM) comes from coupling of the two highest valence bands ($n=3,4$) at the off-Γ k point of Eq. (4) with $j_x=j_y=1$. This large projection shows that this is *not* a surface state despite the fact that the wave function is localized near the surface. Likewise, 70% of the conduction-band minimum (CBM) comes from the lowest two conduction bands at $j_x=j_y=3$. Thus the near-gap states are qualitatively different from simple effective mass depiction [Eq. (5)] in that they represent interband coupling and off-Γ ($j\neq 0$) contributions. The fact that the VBM and CBM wire states project into bulk states of *different wave vectors k* (i.e., different j_x, j_y) proves conclusively that the band gap is *pseudodirect*, not direct.

(ii) *Hydrogen chemisorption changes the localization patterns, polarization, and state densities of the light-emitting levels:* This is illustrated in Fig. 1 where the near band-gap wave function amplitudes $|\psi_f^{\rm wire}(x,y)|^2$, energy level separations, and radiative lifetimes for clean (a) and hydrogen-covered (b) 8×8 Si wire are shown. Three points are noteworthy. First, we see that H chemisorption concentrates more of the VBM and CBM wave-function amplitude toward the interior of the wire. Thus, despite a large surface-to-volume ratio, the band-edge states are expected to reflect the properties of the Si skeleton rather than surface effects. Second, H chemisorption changes the order of states, thus, their expected polarization. For example, the xy-polarized *doublet* constituting the CBM of the wire with free surface is pushed to higher energy and replaced by the z-polarized *singlet* upon chemisorption. Third, the sparsely spaced levels near the VBM and CBM of the clean wire [see the four-level spread of 392 and 369 meV, in Fig. 1(a)] give way to a ~tenfold denser level spacings upon chemisorption [Fig. 1(b)].

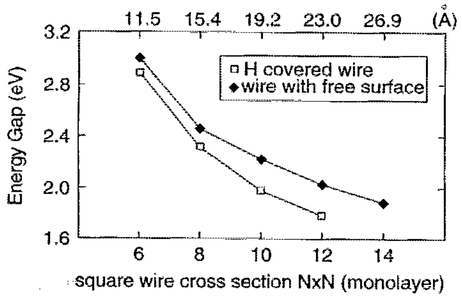

FIG. 2. Dependence of the band gap on the wire size. For the wire with free surfaces we consider only intrinsic states.

(iii) *Chemisorption reduces the band gap:* While quantum confinement increases the band gap as the size is reduced, Fig. 2 shows that hydrogen chemisorption *reduces* the intrinsic band gap. This reflects a combination of level repulsion between Si-like and H-induced states, and the effective increase of wire size (thus, reduced confinement) with hydrogen coverage.

(iv) *The emission spectrum to the states near the* VBM *exhibits bands separated by significant energy gaps:* These are denoted as α, β, and γ in Fig. 3. Band α involves the four highest VBs and four lowest CBs (Fig. 1) and is characterized by a slow average emission lifetime $\tau_{\rm av}=[\Sigma_{i,f}^{N}\tau_{if}^{-1}]^{-1}$ of 0.35 μs. This lifetime increase rapidly as the wire size increase (Fig. 4). The rather long lifetime (small oscillator strength) reflects the *psuedodirect nature* of the wire band gap.[9] We identify this band with the "slow emission" of Calcott[4] *et al.* The β band lies 0.6 eV above the α band (Fig. 3) and has faster transitions with $\tau_{\rm av}=21$ ns. We identify this band with Calcott's "fast emission."

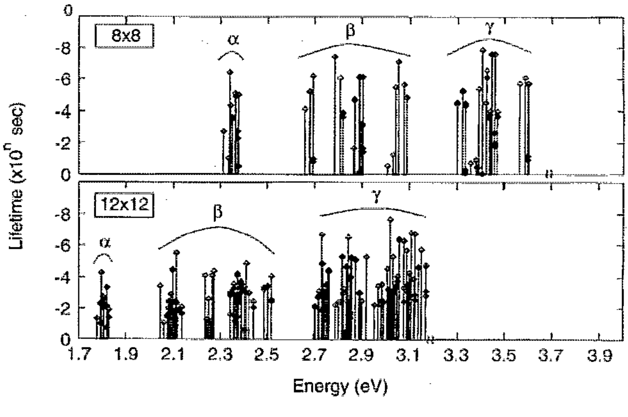

FIG. 3. Calculated radiative transition lifetime from the four highest VB states as functions of the transition energy.

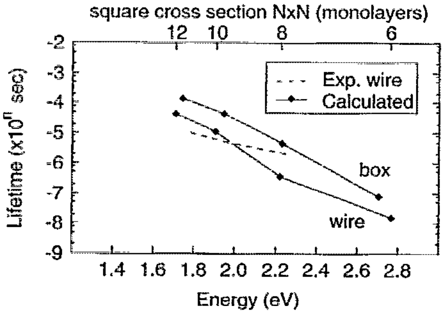

FIG. 4. Comparison of calculated (solid lines) lifetimes of quantum wires and quantum boxes with experimental *S*-band emission in porous Si (see Ref. 4).

(v) *The lifetime versus energy spectrum agree with experiment if a mixture of quantum dots and wires is postulated:* Figure 4 shows that the calculated τ vs ϵ curve shows a faster increase of τ_R with size compared with the measured curve. This means that as size increases the calculated transition become forbidden (i.e., bulklike) faster than the measured one. This could be explained by assuming that porous Si is made of wires *and* boxes. In fact, it is reasonable to imagine that at the beginning of the etching process of porous Si one forms mostly *thick* wires, while after extended etching the wires thin down into *linked-sausage shapes* and eventually some of them break into *quantum boxes.* Thus, the small photon energy region should represent mostly emission from wires (Fig. 4) while the higher photon energy region could represent a larger contribution from boxes. This means that the "effective" τ_R vs ϵ curve should consist of the wire contribution at small ϵ, moving into a box contribution at larger ϵ's. This is a flatter curve than for pure wires.

We would like to thank S. Froyen and L. W. Wang for many helpful discussions on the subject. This work was supported by the U. S. Department of Energy, under Contract No. DE-AC02-83-CH10093.

[1] See many recent articles on porous Si in *Microcrystalline Semiconductors: Materials Science and Devices,* edited by P. M. Fauchet *et al.* (Materials Research Society, Pittsburgh, PA, 1992), Vol. 283.

[2] L. T. Canham, Appl. Phys. Lett. **57**, 1046 (1990).

[3] M. S. Brandt, H. D. Fuchs, M. Stutzmann, J. Weber, and M. Cardona, Solid State Commun. **81**, 307 (1992).

[4] P. D. J. Calcott, K. J. Nash, L. T. Canham, M. J. Kane, and D. Brumheada, J. Phys. Condens. Matter **5**, L91 (1993).

[5] M. B. Robinson, A. C. Dillon, and S. M. George, Appl. Phys. Lett. **62**, 1493 (1993).

[6] V. Petrova-Koch, T. Muschik, A. Kux, B. K. Meyer, F. Koch, and V. Lehmann, Appl. Phys. Lett. **61**, 943 (1992).

[7] L. L. Wang and A. Zunger (unpublished).

[8] See reference inside the letter of A. J. Read, R. J. Needs, K. J. Nash, L. T. Canham, P. D. J. Calcott, and A. Qtiesh, Phys. Rev. Lett. **69**, 1232 (1992).

[9] Inside α band, the band edge transition has a 2.2 ms lifetime and is 26 meV below the next transition. This happens to be close to the very slow transition of 3 ms with a 20 meV energy separation detected and designated as spin-triplet transition by Ref. 4, although spin-degree of freedom is not considered in the present calculation.